Ferroelastic domains and mechanical hysteresis in the crystal of p-(trimethylammonium) benzenesulphonate zwitterion

1999 J. Phys.: Condens. Matter 11 5797

(http://iopscience.iop.org/0953-8984/11/30/310)

J. Phys.: Condens. Matter **11** (1999) 5797–5810. Printed in the UK PII: S0953-8984(99)00266-0

Ferroelastic domains and mechanical hysteresis in the crystal of p-(trimethylammonium) benzenesulphonate zwitterion

J Even†, M Bertault†, L Toupet† and W J Kusto‡

† Groupe Matière Condensée et Matériaux, UMR 6626 au CNRS, Université de Rennes I, Campus de Beaulieu, F-35042 Rennes Cédex, France

‡ Institute of Physical and Theoretical Chemistry, Technical University of Wroclaw, 50-370 Wroclaw, Poland

Received 22 December 1998

Abstract. The crystal of p-(trimethylammonium) benzenesulphonate (ZWT) undergoes a first order ferroelastic phase transition at about $T_3 = 386$ K. It yields a tetragonal γ-phase at higher temperature when going from the orthorhombic β-phase at lower temperature. By using experimental techniques such as x-ray diffraction, dilatometry and optical birefringence, ferroelastic domains have been displayed and studied at room and at higher temperature in the β structural phase, and in the temperature range which surrounds the transition at T_3. A reversible change of the orientation of the domains is observed when a uniaxial pressure is applied at increasing and decreasing temperatures. Coexistence of domains with structures characteristic of the orthorhombic β-phase and of the tetragonal γ-phase has been observed around the transition temperature T_3.

(Some figures in this article appear in colour in the electronic version; see `www.iop.org`)

1. Introduction

A single crystal of methyl p-dimethylaminobenzenesulphonate (MSE) can be converted by a thermally induced methyl-transfer reaction to the zwitterionic product p-(trimethylammonium) benzenesulphonate (ZWT) [1–9]. By another method, ZWT single crystals of good quality have been obtained by very slow evaporation of a water solution of the ZWT compound [10]. Phase transitions are observed in the ZWT crystal and crystallographic structures of the corresponding phases have been studied at low and high temperatures [3, 10]. Two orthorhombic phases have been then determined, one α-phase with the $Pnc2$ space group at $T < 291$ K [3, 10] and one β-phase with the $Pca2_1$ space group at 307 K $< T <$ 386 K [10]; an intermediate phase exists between two phase transitions which have been observed at $T_1 = 291$ K and $T_2 = 307$ K [10]. The phase transition which takes place at $T_3 = 386$ K yields a tetragonal γ-phase with the $P4_2/ncm$ space group at $T > T_3$. Study of the thermal anomaly observed by scanning microcalorimetry (DSC) shows that the orthorhombic to tetragonal phase transition at T_3 is of first order. It corresponds to a transition from the $4/mmm$ high temperature point group to the $mm2$ low temperature point group with improper spontaneous strain: two types of ferroelastic domain (1 and 2) are predicted in the low temperature phase by theoretical works [10, 11]. An orientational disorder of the $N(CH_3)_3^+$ and SO_3^- groups of the ZWT molecules is observed at temperatures $T > T_3$. The molecular dipolar axis of the ZWT molecule remains parallel to the c crystallographic axis of the tetragonal γ-phase. The spontaneous strains which take place in the ZWT crystal appear at $T < T_3$ only in the (a,

0953-8984/99/305797+14$30.00

b)-plane of the tetragonal γ-phase [10]. The *c*-axis (molecular dipolar axis) of the tetragonal high temperature γ-phase corresponds to the *b*-axis of the orthorhombic intermediate β-phase and to the *c*-axis of the orthorhombic low temperature α-phase [10]. In this paper, we have decided to adopt for the three structural α-, β- and γ-phases of the ZWT crystal the notations used for the low temperature α-phase: the *c*-axis will be the molecular dipolar axis and the *a*- and *b*-axes will define the two other crystallographic axes of the orthorhombic cells in the α- and β-phases. In that case the volume of the cell chosen for representing the high temperature γ-phase will be twice as big as the volume of the primitive cell.

We present in this paper the results which have been obtained from the experimental study of the strains taken into account in the previous paragraph. By using x-ray diffraction, dilatometry (TMA) and optical birefringence on ZWT single crystals, we have been able to measure the lattice distortion (spontaneous strain) as a function of temperature, to observe the two predicted ferroelastic domains near room temperature and to find evidence of mechanical hysteresis by applying uniaxial mechanical pressure. The experimental methods are described in section 2. In part 3, the lattice distortion is studied by x-ray diffraction. Dilatometric measurements are given in part 4 and optical observations described in part 5. Section 6 is a discussion and a conclusion.

2. Experimental methods

2.1. Crystal growth

MSE crystals were thermally reacted to complete transformation into ZWT (usually by isothermal annealing at about 350–360 K) and then dissolved in very pure water. After filtration, ZWT crystals were grown by very slow evaporation of the water solution (about ten days) at room temperature. The crystals obtained were colourless (001) plates of maximum thickness $\sim$0.5 mm.

2.2. X-ray diffraction

X-ray diffraction studies were performed with an Enraf-Nonius CAD-4 diffractometer [12]. The high temperature measurements were obtained by setting the crystal in a dry air flow controlled (to within 0.5 K) by a thermal resistance. For each measurement at stabilized temperature, 30 Bragg peaks were collected and refined to lead to the values of the *a*, *b*, *c* crystallographic parameters.

2.3. Dilatometric measurements

Dilatometric experiments were performed with a Perkin-Elmer dynamic mechanical analyser DMA 7 used in static thermomechanical mode (TMA) with a 10 K min^{-1} scanning rate for heating and cooling measurements. A static force (uniaxial pressure) equal to 20 mN was applied to a quartz probe of 1 mm diameter. The measurement head of the DMA 7 was flushed with pure nitrogen gas and its temperature was stabilized by circulating cold water–ethanol from a thermostatic bath controlled at 280 ± 0.1 K. The temperature is measured by a chromel–alumel thermocouple with a precision of ± 2 K. The displacement sensitivity is equal to ± 0.05 μm. The probe was applied along directions parallel to the three crystallographic axes *a*, *b*, *c*, after the crystal orientation had been determined by conoscopic measurements with a polarized light microscope.

2.4. Optical birefringence

Orthoscopic and conoscopic observations were performed with a polarized light microscope Laborlux 12 pol Leitz [13, 14]. For high temperature measurements at about $T_3 = 386$ K, it was equiped with a Linkham TMS90 heating system having a temperature stability equal to ± 0.1 K. The ZWT crystals were always observed along a direction parallel to the crystallographic c fourfold axis of the tetragonal γ-phase; this is perpendicular to the faces of the as-grown ZWT plates and corresponds to the ex-b crystallographic axis of the orthorhombic β-phase.

3. Lattice distortion

We have observed that the directions of the a and b crystallographic axes of the orthorhombic β-phase correspond respectively to the directions of the a and b crystallographic axes of the tetragonal γ-phase when (see the introduction) we adopt for the three structural α-, β- and γ-phases the notations used for the low temperature α-phase.

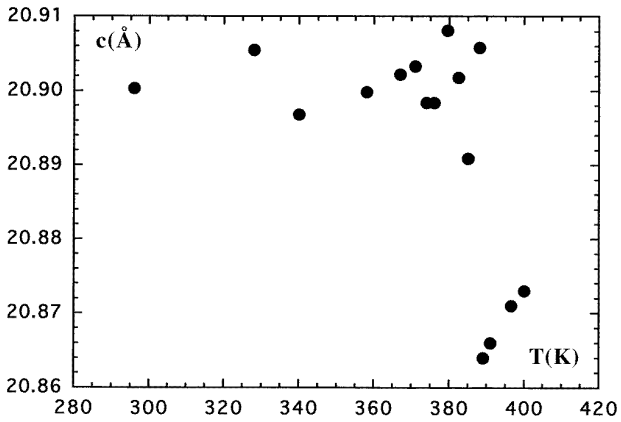

Figure 1. Evolution, as a function of temperature in the [280–420 K] temperature range, of the c crystallographic cell parameter measured in a ZWT single crystal by x-ray diffraction.

Figure 1 shows the variation (obtained by x-ray diffraction) of the c-parameter as a function of temperature in the [280–420 K] temperature interval. It undergoes a very small ($\Delta c/c \approx -0.15 \pm 0.08\%$) but discontinuous decrease at $T = T_3$. When using the complete structural determinations made at $T = 375$ K (in the β-phase) and at $T = 400$ K (in the γ-phase), a value of $\Delta c/c \cong -0.08 \pm 0.08\%$ is obtained [10]. These results are close to the experimental precision of the apparatus but they are consistent with the results of the dilatometric study made in the direction of the c-axis (section 4).

In figure 2, the variation of a- and b-parameters (obtained by x-ray measurements) as a function of temperature are represented in the [320–420 K] temperature range. A very small decrease ($\Delta a/a = -0.06\%$) of the a-parameter is observed at the transition temperature T_3 together with a strong increase ($\Delta b/b \cong +4.5\%$) of the b-parameter. Some information about the evolution of the order parameter may be deduced from the variation of a and b near the transition: this is discussed in the conclusion (see section 6). At $T > T_3$, the a- and b-parameters are equal to the same value, 10.175 Å. This is the single value 7.195 Å (obtained when the structure determination of the tetragonal γ-phase was performed at $T = 400$ K [10])

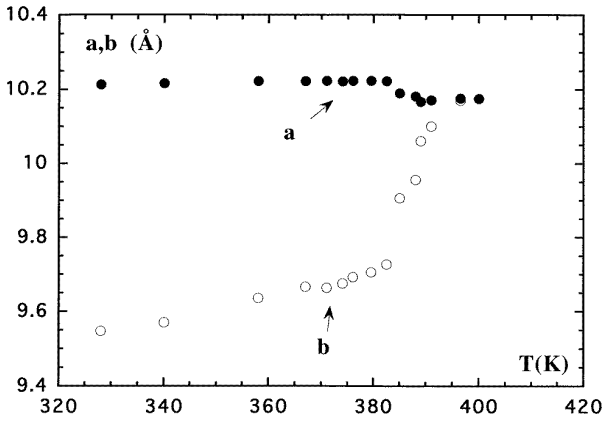

Figure 2. Evolution, as a function of temperature in the [320–420 K] temperature range, of the a and b crystallographic cell parameters measured in a ZWT single crystal by x-ray diffraction. For temperatures higher than $T_3 = 386$ K, the values of a- and b-parameters are equal to the unique value of $a = b$ cell parameter of the tetragonal γ-phase.

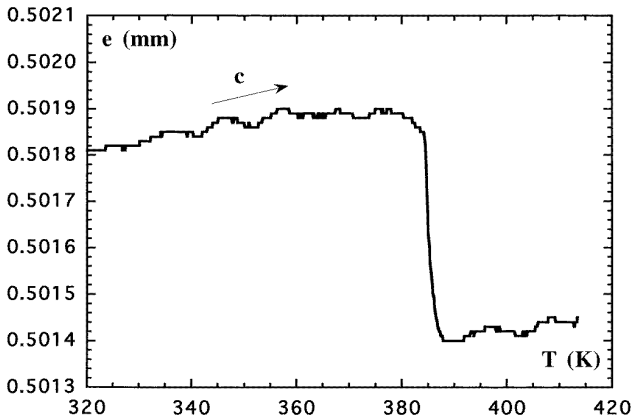

Figure 3. Evolution, as a function of temperature in the [320–420 K] temperature range, of the ZWT single crystal e dimension oriented in a direction parallel to the c crystallographic axis. The measurements were performed by dilatometry on increasing the temperature at a scanning rate of 10 K min^{-1}.

after being multiplied by a factor equal to $\sqrt{2}$. This is done to account for the cell halving and the 45° angle of the tetragonal unit cell with respect to the orthorhombic cell. One may notice that there is also a strong and discontinuous volume increase ($\Delta V/V \cong +3.7\%$) at T_3.

4. Dilatometric measurements

Figure 3 shows the evolution of the thickness e for an as-grown ZWT crystal plate as a function of temperature in the [320–420 K] interval with increasing temperature when applying the probe along the c crystallographic axis (perpendicular to the plate). A small and discontinuous

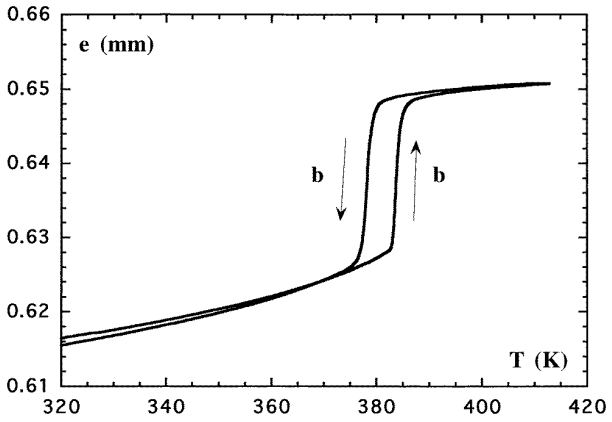

Figure 4. Evolution, as a function of temperature in the [320–420 K] temperature range, of the ZWT single crystal dimension e oriented in a direction parallel to the b crystallographic axis. The measurements were performed by dilatometry, first, when increasing the temperature at a scanning rate of 10 K min^{-1} and, second, when decreasing the temperature at a scanning rate of 10 K min^{-1}.

decrease is observed at $T = T_3$ ($\Delta e/e \cong -0.10 \pm 0.02\%$) in agreement with the x-ray diffraction measurements (figure 1). When applying the probe along a direction parallel to the b crystallographic axis, the evolution of the crystal width e as a function of temperature in the [320–420 K] temperature interval is shown in figure 4 with increasing and decreasing temperatures; we see that the evolution with increasing temperature can be compared to the previous x-ray diffraction measurements (figure 2) showing a strong increase of e at T_3. On the other hand the large hysteresis ($\cong$5 K) observed for the evolution of e in the temperature range which surrounds the transition with increasing then decreasing temperature is related to the value of the scanning rate (10 K min^{-1}) used in the TMA experiment. The hysteresis has really a value of about 0.4 K for the first order transition as observed in the birefringence study [10].

The most striking differences were observed when applying the probe along a direction parallel to the a crystallographic axis. In a first case, when the probe was applied by smashing the crystal surface, the curve representing the variation of the width as a function of temperature was strictly identical to the curve obtained when the probe was applied along a direction parallel to the b crystallographic axis (figure 4). Conoscopic measurements (section 5), made just after the dilatometric experiment, confirmed that the crystallographic a- and b-directions had undergone a 90° rotation.

In a second case, when the probe was applied carefully (slowly enough) on the surface of the crystal parallel to the (a, b)-plane, a partial decrease of the width was observed when increasing the temperature in the range extending below the transition temperature T_3 (figure 5): this indicates that some parts of the crystal had already made an $a \rightarrow b$ change in the orientation of the crystallographic axes. Consequently, the b-like step was only partial at T_3 when increasing the temperature but a full step (identical to the one observed in figure 4) was observed with decreasing temperature: this is in agreement with the fact that the conoscopic measurements showed a full $a \rightarrow b$ change in the orientation of the crystallographic axes at the end of the TMA experiment.

In a third case, we may notice that the crystalline orientations only changed at T very near T_3 when increasing the temperature (figure 6): so, on the same experimental curve, we may

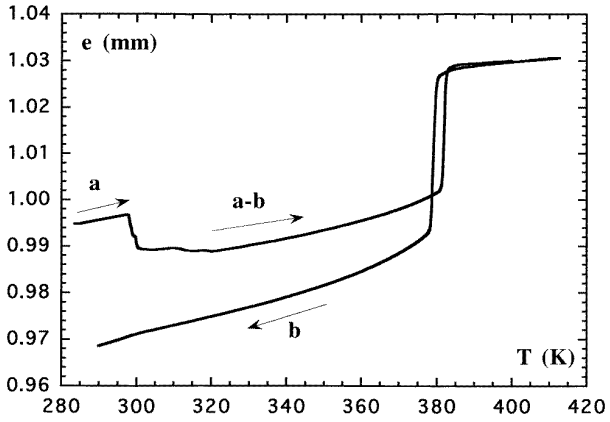

Figure 5. Evolution, as function of temperature in the [280–420 K] temperature range, of the ZWT single crystal dimension e oriented, at the beginning of the experiment, in a direction parallel to the a crystallographic axis. The measurement was performed by dilatometry, first, when increasing the temperature at a scanning rate of 10 K min^{-1} and, second, when decreasing the temperature at a scanning rate of 10 K min^{-1}. Some parts of the crystal undergo an $a \rightarrow b$ change of orientation at about $T = 300$ K. On recording with decreasing temperature, the whole crystal is a single domain in which the a-axis at the beginning of the experiment becomes the b-axis.

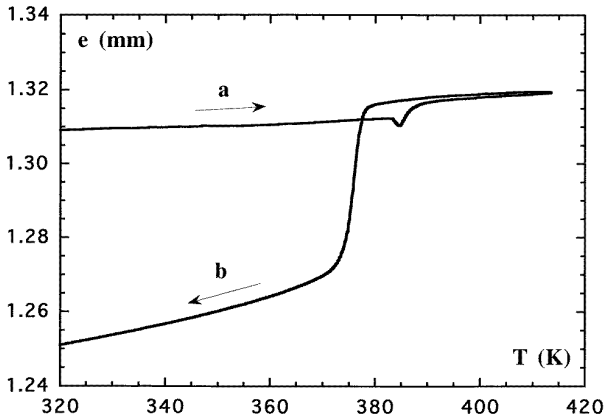

Figure 6. Evolution, as a function of temperature in the [320–420 K] temperature range, of the ZWT single crystal dimension e oriented, at the beginning of the experiment, in a direction parallel to the a crystallographic axis. The measurement was performed by dilatometry, first, when increasing the temperature at a scanning rate of 10 K min^{-1} and second, when decreasing the temperature at a scanning rate of 10 K min^{-1}. The sample dimension e has a temperature evolution corresponding to the a crystallographic direction on increasing the temperature up to the transition temperature $T_3 = 386$ K. When decreasing the temperature, the sample dimension e has a temperature evolution corresponding to the b crystallographic direction. The orientations of the crystallographic axes have changed as checked by optical birefringence ($a \rightarrow b$ and $b \rightarrow a$).

observe at the same time a result characteristic of the a-direction (figure 2) on the part recorded with increasing temperature and a result characteristic of the b-direction when decreasing the

temperature (figure 4) on the part recorded with decreasing temperature. The reverse $b \rightarrow a$ change of orientation was never observed in our experiments. This indicates clearly that the uniaxial pressure exerted on the ZWT crystal when applying the probe always stabilizes the ferroelastic domains which are observed when the direction of the smaller crystallographic axis ($b < a$) is parallel to the probe.

5. Optical birefringence

In the range surrounding the transition temperature $T_3 = 386$ K, the orthorhombic to tetragonal $\beta \rightarrow \gamma$ phase transition of ZWT crystals may be conveniently studied by optical birefringence for three reasons. First, the crystals of orthorhombic symmetry are optically biaxial and the crystals of tetragonal symmetry are optically uniaxial. Second, ZWT crystals of good quality are colourless (001) plates. The optical axis is then perpendicular to the (a, b)-plane (parallel to faces of the plates) in which the changes of orientation of the crystallographic axes occur. Third, the phase transition at T_3 is of first order. For temperatures $T < T_3$ the birefringence Δn_{ab} has a value equal to at least 26×10^{-4} [10]. Then the interference figure clearly shows the orientations of the a- and b-axes when the observation direction of the polarized light microscope is perpendicular to faces of the ZWT plates.

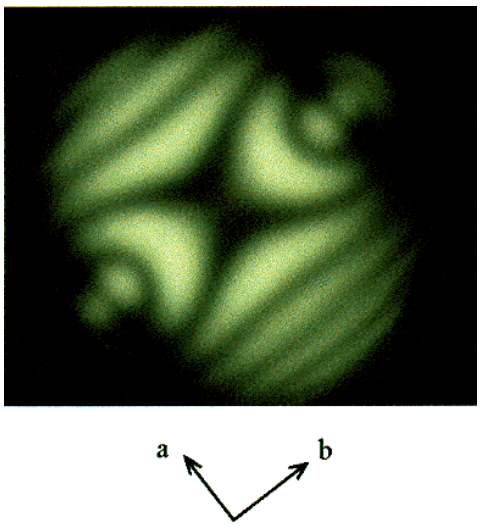

Figure 7. Conoscopic picture with green filter recorded at $T = 383.1$ K when the observation axis of the polarized microscope has a direction parallel to the c fourfold axis of the tetragonal γ-phase. The a and b crystallographic directions are deduced from the interference figure corresponding to an orthorhombic optically biaxial crystal. The notations of the low temperature α-phase are used for the crystallographic axes [10].

Figures 7 and 8 show two conoscopic pictures recorded at temperatures near the transition temperature T_3, the first at $T = 383.1$ K ($T < T_3$) and the second at $T = 387.0$ K ($T > T_3$). The structural change as observed by birefringence is very rough, but within a range of a few tenths of a degree ($\widehat{=}0.5$ K) coexistence of high temperature and low temperature phase domains is observed by orthoscopic observations. For example we can see with increasing temperature in this range (2 K min^{-1}) the progression of the high temperature domain boundaries to the

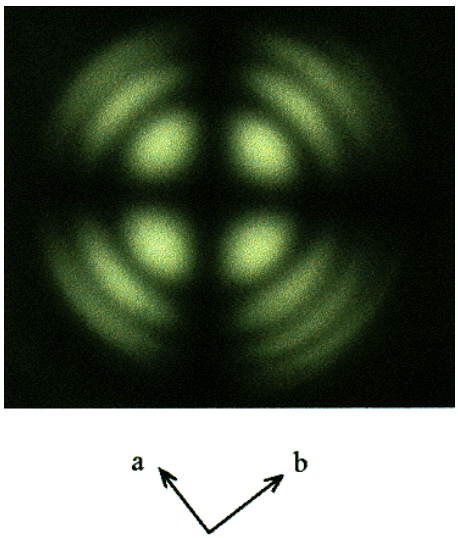

Figure 8. Conoscopic picture with green filter recorded at $T = 387$ K when the observation axis of polarized microscope has a direction parallel to the c fourfold axis of the tetragonal γ-phase. The interference figure corresponds to a tetragonal optically uniaxial crystal. The a and b crystallographic directions in the orthorhombic β-phase (figure 7) are shown on the picture for comparison.

detriment of the low temperature domains; the inverse situation is observed with decreasing temperature. The orientations of a and b crystallographic axes are easily determined at $T < T_3$ as shown in figure 7 for $T = 383.1$ K.

In figure 9 two ferroelastic domains 1 and 2 (as predicted in [11]) are observed on the same orthoscopic picture recorded at room temperature: in each of them there are two different orientations of the a and b crystallographic axes making an angle of 90 degrees. They correspond to two distinct regions, the darker 1 extending inside the central square and the clearer 2 outside and all around the square. We may note that the domain wall makes an angle of 45 degrees with the a- and b-directions in both domains. A uniaxial pressure was then applied at room temperature on two opposite sides of this approximately rectangular crystal in a direction which corresponds to that of the a crystallographic axis in the central 'dark' domain and to that of the b axis in the clearer region outside the square: the result of this stress is that one single domain with a- and b-orientations of domain 2 was only observed under pressure and after pressure was removed. The ferroelastic domain corresponding to the central square in figure 9 has undergone a 90° rotation of the a and b crystallographic axes around the c-axis.

It may be noted that cracks had appeared in the crystal after removing pressure, corresponding mostly to cleavage planes. It was possible to induce again the $a \rightarrow b$ change of orientation by applying the uniaxial pressure in a direction perpendicular to the previous direction, for example on the two other opposite sides of the crystal. However the same crystal may usually not be used for more than two or three sequences of successive 90° rotations of the crystallographic axes. We have then not been able to make a quantitative determination of the mechanical hysteresis because of the crystal fragility. The cracks appearing in the crystal are probably related to defects but also to the fact that the strains are discontinuous and very strong at the $\beta \rightarrow \gamma$ first order transition (see sections 3 and 4, and [11]).

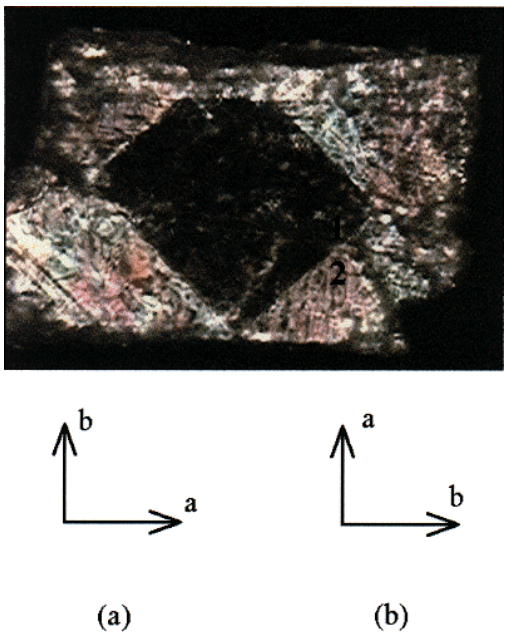

Figure 9. Orthoscopic picture recorded at room temperature when the observation axis of the polarized microscope has a direction parallel to the c fourfold axis of the tetragonal γ-phase. Two ferroelastic domains of types 1 and 2 are observed: they correspond to the regions darker inside and clearer outside the central square. Inside the central square the a and b crystallographic directions correspond to case (a) and outside the central square to case (b): these directions make respectively an angle of 90 degrees in both domains.

6. Discussion and conclusion

X-ray diffraction, dilatometric and optical birefringence studies have confirmed that the structural phase transition $\beta \leftrightarrow \gamma$ which takes place at $T_3 = 386$ K in ZWT crystals is a ferroelastic first order transition. The two types of domain 1 and 2 predicted by theoretical works [10, 11] are observed in the low temperature β-phase by optical polarized microscopy. The mutual correspondence between the two types of domain at temperatures $T < T_3$ is a simultaneous 90° rotation of the a and b crystallographic axes (when keeping the notations of the α-phase, as indicated in section 1). This rotation of the a- and b-axes may be induced by a uniaxial pressure applied along the largest unit cell parameter a ($a = 10.198$ Å, $c = 9.648$ Å at $T = 333$ K and $a = 10.224$ Å, $c = 9.801$ Å at $T = 375$ K, by using the notations of the low temperature α-phase). Moreover, optical microscopy has shown that the domain wall between domains 1 and 2 observed in the low temperature β-phase at temperature $T < T_3$ makes an angle of about 45 degrees with the directions of the a and b crystallographic axes of the orthorhombic β-phase. At the transition temperature T_3, a coexistence of low temperature orthorhombic domains and high temperature tetragonal domains is observed. The domain wall is still oriented in a direction making about a 45° angle with the directions of a and b crystallographic axes. When the temperature is slowly increased from a temperature very slightly below T_3 (or decreased from a temperature slightly above T_3) the domain wall moves in keeping the same orientation.

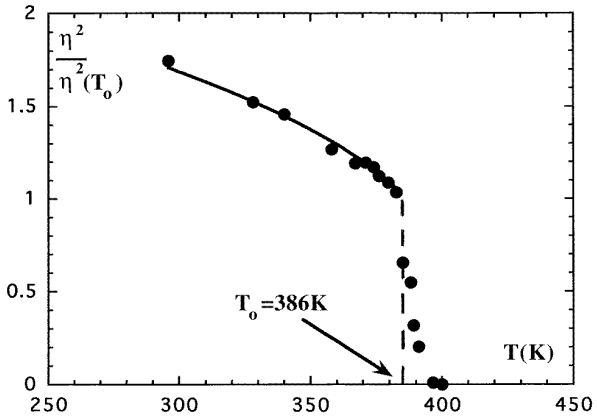

Figure 10. Evolution of $[e_1+e_2(T)]/[e_1+e_2(T_0)]$ as a function of temperature (dark circles). The dark line corresponds to the fit by the theoretical expression

$$\frac{\eta^2}{\eta^2(T_0)} = \frac{2}{3}\left[1+\sqrt{\frac{\frac{4}{3}T_0 - T_c/3 - T}{\frac{4}{3}(T_0-T_c)}}\right] \qquad (T < T_0)$$

by taking $T_c = 355$ K and $T_0 = 386$ K.

Information about the order parameter evolution as a function of the temperature may be obtained from the variations of the lattice parameter near the transition at T_3 (see section 3). When considering the $P4_2/ncm$ space group of the high temperature γ-phase ($4/mmm$) and the $Pca2_1$ space group of the low temperature β-phase ($mm2$), one may conclude that the (e_1+e_2) and e_3 deformations are coupled to the order parameter in the Landau potential by linear–quadratic terms ($e_3\eta^2$ and $(e_1+e_2)\eta^2$) [11]. As a result (e_1+e_2) and e_3 should vary proportionally to η^2. The Landau 2–4–6 potential looks like $F = F_0 + (a/2)(T-T_c)\eta^2 + B\eta^4 + C\eta^6$ with a negative B term; if one calls $\eta^2(T_0)$ the step of the square of the order parameter at the transition temperature T_0, it follows that $\eta^2 = \frac{2}{3}\eta^2(T_0)[1+\sqrt{(\frac{4}{3}T_0 - T_c/3 - T)/\frac{4}{3}(T_0-T_c)}]$ (for $T < T_0$).

Figure 10 represents the variation of $[e_1+e_2(T)]/[e_1+e_2(T_0)]$ as a function of temperature when $e_1+e_2 = (a+b-2a_{HT})/a_{HT}$ is normalized by $e_1+e_2(T_0)$. The fit of the experimental results by the theoretical expression $\eta^2/\eta^2(T_0) = \frac{2}{3}[1+\sqrt{(\frac{4}{3}(T_0) - T_c/3 - T)/\frac{4}{3}(T_0-T_c)}]$ ($T < T_c$) is represented by the dark line and yields $T_c = 355$ K. Due to existence of few experimental data, we point out that this result should be confirmed by other measurements of the $\eta^2(T)$ variation. The difference $T_0 - T_c$ is equal to $3B^2/16aC$ when it is calculated by using the Landau 2–4–6 potential. Other relations between the a-, B-, C-parameters may be obtained from experimental measurements of thermodynamic quantities like the heat of transition $\Delta Q = 3aBT_0/8C$ and the specific heat jump at T_0, $\Delta C_p = -a^2T_0/B$. A combination of the theoretical expressions of (T_0-T_c), ΔQ and ΔC_p yields $\Delta Q/\Delta C_p(T_0-T_c) = 2$. It is then possible to calculate $\Delta C_p = \Delta Q/2(T_0-T_c) = 0.31$ J g^{-1} K^{-1} from $T_0 - T_c = 31$ K and $\Delta Q = 19.2$ J g^{-1} [10]. Further experimental work would be interesting in order to obtain a more precise description of the transition, in particular on the coupling between the strains and the order parameter [11].

It is possible to propose an interpretation of the domain wall orientation by considering the positions of the ZWT molecules in a schematic representation of the unit crystallographic

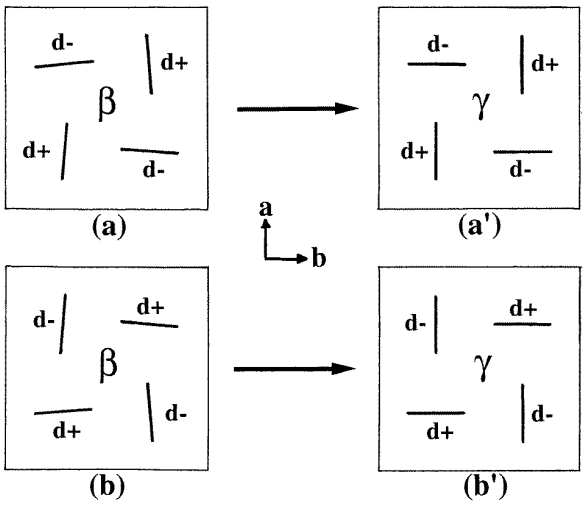

Figure 11. Schematic representation of the unit crystallographic cells of the β- and γ-phases of the ZWT crystal in the (a, b)-plane. d+ (electric dipole up) and d− (electric dipole down) along the c crystallographic axis perpendicular to the (a, b)-plane and segments of line (projections of the phenyl rings in the (a, b)-plane) define respectively the orientations and shapes of the ZWT molecules. The eight molecules in the same unit cell are arranged in upper and lower layers parallel to the (a, b)-plane and named (a) and (b) in the β-phase, (a′) and (b′) in the γ-phase.

cells in the β- and γ-phases (figure 11). First, we consider the packing in the orthorhombic β-phase: it corresponds to an antiferroelectric array of the d+ (dipole up) and d− (dipole down) ZWT molecules which are perpendicular to the (a, b)-plane (as shown in [10]). Along one stack parallel to the c-axis, all molecules have the same dipolar orientation, either d+ or d−, respectively in the same and in the opposite directions to the c-axis. Second, the phenyl ring orientations are also very important: they are drawn in figure 11 as segments of line which represent the projections of the phenyl rings on two successive layers (parallel to the (a, b)-plane) in the same unit cell. The upper and the lower layers are named (a) and (b) in the β-phase ($T < T_3$) and they yield respectively the corresponding (a') and (b') layers in the γ-phase ($T > T_3$). In the β-phase and for the upper layer (figure 11(a)) for example, the phenyl ring orientations are almost the same for all d+ molecules (they make an angle of ± 5 degrees compared with the direction of the a-axis); this is also the case for the phenyl ring orientations of the d− molecules compared to the direction of the b-axis. Then one can see that the mean static orientation of the phenyl rings of d+ molecules is perpendicular to the mean static orientation of the phenyl rings of d− molecules. The same description holds also for the tetragonal γ-phase: the orientations of the phenyl rings of d+ and d− molecules are mean dynamic directions [10] which are perpendicular respectively to the directions of a and b crystallographic axes in both upper and lower layers. In each of the two crystallographic phases, when going from the upper layer to the lower layer by a translation of half the c crystallographic axis, the mean orientations of the phenyl rings for either d+ or d− molecules are rotated by a 90° angle.

To explain the fact that the domain walls are observed either at room temperature (and above) in the β-phase or at $T \cong T_3$ during the $\beta \leftrightarrow \gamma$ ferroelastic phase transition, we

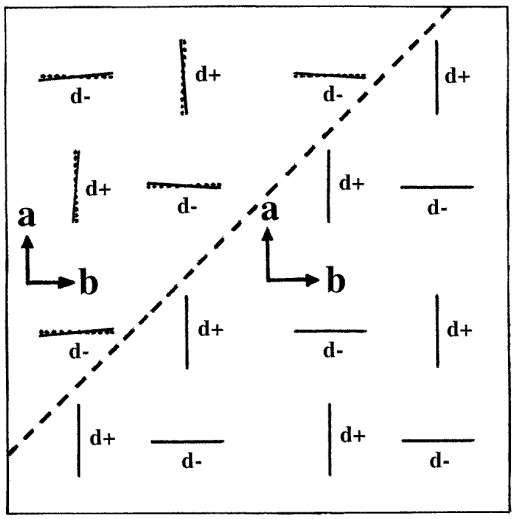

Figure 12. Schematic representation of a domain wall (dashed line) dividing two orthorhombic domains of types 1 and 2 in the β-phase of a ZWT crystal. The domain wall makes an angle of about 45 degrees in relation to the a- and b-axes of the unit cell. The lattice of the type 2 orthorhombic domain is translated parallel to the direction of the c crystallographic axis by $c/2$ in relation to the type 1 orthorhombic domain. This translation may correspond to a stacking fault in the crystal.

propose a geometric schematic construction in the two cases. First consider a domain wall dividing two orthorhombic domains in the β-phase, one of type 1 and the other of type 2. In figure 12 is drawn a geometric construction (deduced from figure 11) showing coexistence of the two types of domain with a domain wall making an angle of about 45 degrees in relation to a and b crystallographic axes. We assume that such a configuration may be obtained by translating the lattice of the type 2 orthorhombic domain by half the crystallographic c-axis in the c-direction in relation to the type 1 orthorhombic domain. We must recall that the a and b crystallographic axes of a type 1 domain are perpendicular to the corresponding a- and b-axes of a type 2 domain. This schematic construction preserves the antiferroelectric array in the (a, b)-plane and a mean 90° angle between the phenyl ring orientations for the d+ and d− molecules (figure 12). Moreover we may also recall that the two types of domain coexist mainly in ZWT crystals of poor quality when ZWT crystals of good quality are made with a single domain. In conclusion, we may say that the defects seem to play an important role for the pinning of the domain walls existing in the β-phase. The presence of these defects can also explain the experimental observation that the domain walls remain motionless when increasing or decreasing the temperature in the β-phase. We may add that the orientations of these domain walls (making an angle of 45 degrees with the directions of a- and b-axes), when they are induced by a stacking fault, are determined by the relation (described previously) between the lattices of the two types of domain (figure 13).

Second, consider now a domain wall dividing a domain with a structure characteristic of the tetragonal γ-phase and a domain with the structure of the orthorhombic β-phase. It is also possible to make a geometric schematic construction showing coexistence of the two types of domain with a domain wall making an angle of about 45 degrees in relation to a and b

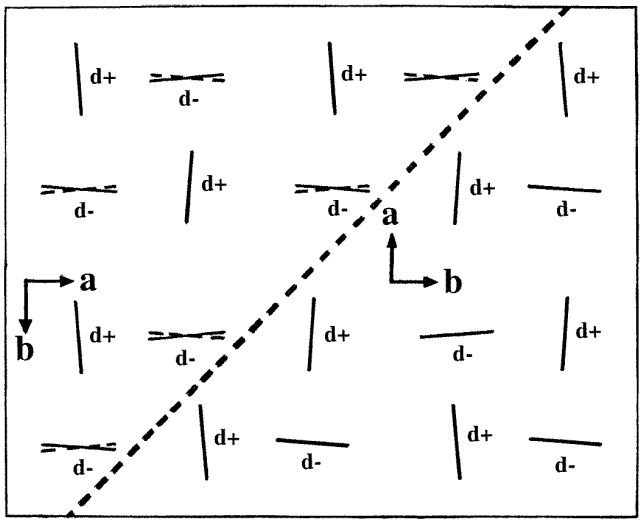

Figure 13. Schematic representation of a domain wall (dashed line) dividing the same layer of ZWT molecules parallel to the (a, b)-plane in the structural β- and γ-phases of a ZWT crystal.The domain wall makes a 45° angle with the a and b crystallographic axes of the β-phase unit cell and of the cell chosen for representing the γ-phase (its volume is twice as big as the one of the unit cell [10]).

crystallographic axes (figure 13): this configuration, which connects a layer (upper or lower) in the unit cell of the orthorhombic β-phase with the corresponding layer in the unit cell of the tetragonal γ phase, preserves the antiferroelectric array in the (a, b)-plane and the 90° angle between the mean orientations of the phenyl rings for d+ and d− molecules. We must recall that the a and b crystallographic axes have the same orientations in the two structural β- and γ-phases (see section 3). In the temperature range near the transition temperature T_3, in which is observed the coexistence of orthorhombic and tetragonal domains (section 5), the domain walls easily move when increasing or decreasing slowly the temperature: this is an indication that the role of defects is in that case less important than in the case of the domains of types 1 and 2 observed in the orthorhombic β-phase. The 45° orientation of the domain walls corresponds to the same orientation of the a and b crystallographic axes of the unit cell of the tetragonal γ-phase in relation to the corresponding a- and b-axes of the unit cell of the orthorhombic β-phase.

References

[1] Sukenik C N, Bonapace J A P, Mandel N S, Lau P Y, Wood G and Bergman R G 1977 *J. Am. Chem. Soc.* **99** 851
[2] Sarma J A R P and Dunitz J D 1990 *Acta Crystallogr.* B **46** 780
[3] Sarma J A R P and Dunitz J D 1990 *Acta Crystallogr.* B **46** 784
[4] Even J, Bertault M, Girard A, Délugeard Y and Marqueton Y 1997 *Chem. Phys. Lett.* **267** 585
[5] Even J, Bertault M, Gallier J, Girard A, Délugeard Y and Kusto W J 1997 *Chem. Phys. Lett.* **279** 319
[6] Even J, Bertault M, Gallier J, Girard A, Délugeard Y, Ecolivet C, Beaufils S, Toupet L and Kusto W J 1998 *Mol. Cryst. Liq. Cryst.* **313** 135
[7] Bertault M and Even J 1998 *Mol. Cryst. Liq. Cryst.* **313** 315
[8] Oda M and Sato N 1997 *Chem. Phys. Lett.* **275** 40
[9] Boerio-Goates J, Artman J I and Gold D 1987 *J. Phys. Chem. Solids* **48** 1185

[10] Even J, Bertault M, Toupet L, Girard A and Kusto W J *Eur. Phys. J.* B at press
[11] Salje E K H 1993 *Phase Transitions in Ferroelastic and Co-elastic Crystals (Cambridge Topics in Mineral Physics and Chemistry)* (Cambridge: Cambridge University Press)
[12] Enraf-Nonius 1977 *CAD-4 Operations Manual* (Delft: Enraf-Nonius)
[13] Rochow T G and Tucker P A 1994 *Introduction to Microscopy by Means of Light, Electrons, X-Rays or Acoustics* (New York: Plenum)
[14] Kusto W J, Rivera J P and Schmid H 1992 *Ferroelectrics* **125** 191